



Available online at [www.sciencedirect.com](http://www.sciencedirect.com)

**ScienceDirect**

Procedia Engineering 143 (2016) i

---

---

**Procedia  
Engineering**

---

---

[www.elsevier.com/locate/procedia](http://www.elsevier.com/locate/procedia)

## **Advances in Transportation Geotechnics III**

*Guest Editor:*

*António Gomes Correia*

## Contents

An Application of Pulsed Power Technology and Subcritical Water to the Recycling of Asphalt Concrete R.I.H.D.T. Amoussou, M. Sasaki, M. Shigeishi .....	1
The Effect of Granulation Time of the Pan Granulation on the Characteristics of the Aggregates Containing Dunkirk Sediments H. Azrar, R. Zentar, N.-E. Abriak .....	10
Full-scale Evaluation in a Fatigue Track of a Base Course Treated with Geopolymers J. Camacho-Tauta, O. Reyes-Ortiz, A.V. da Fonseca, S. Rios, N. Cruz, C. Rodrigues .....	18
Hydrophobic Polymer Additive for Stabilization of Aggregates in Local Government Roads D. Cameron, C. Hopkins, M. Rahman .....	26
Effect of Geosynthetic Reinforcement Inclusion on the Strength Parameters and Bearing Ratio of a Fine Soil D.M. Carlos, M. Pinho-Lopes, M.L. Lopes .....	34
Permanent Deformation Behavior of a Cement-modified Base Course Material S. Chummuneerat, P. Jitsangiam .....	42
Geotechnical and Geoenvironmental Assessment of Recycled Construction and Demolition Waste for Road Embankments N. Cristelo, C.S. Vieira, M. de Lurdes Lopes .....	51
Influence of Water Content in the UCS of Soil-cement Mixtures for Different Cement Dosages D. Ribeiro, R. Néri, R. Cardoso .....	59
Strength of Non-traditional Granular Materials Assessed from Drained Multistage Triaxial Tests S.M. Reis Ferreira, A.G. Correia, A.J. Roque .....	67
Mechanical Behavior of Soil Cement Blends with Osorio Sand M. Forcelini, G.R. Garbin, V.P. Faro, N.C. Consoli .....	75
Main Results of the Questionnaire for Portuguese Entities Potential Users of Construction and Demolition Recycled Materials (C&DRM) A.C. Freire, I.M. Martins, C. Ferreira, J. Gonçalves, A.J. Roque, I. Pinto .....	82
Organic-mineral Aggregate for Sandy Subsoil Strengthening J. Gayda, A. Ayzenshtadt, A. Tutugin, M. Frolova .....	90
A New Granulation Method with the Process of Crumbling Partially-cemented Liquid Muds and its Application to a Motocross Track K. Hayano, H. Yamauchi, N. Wakuri, S. Tomiyoshi .....	98
Study on Physicochemical Properties and its Effective Use of Asphalt Pavement Cutting Waste Water K. Hayano, A. Matsumoto .....	104
Tensile Strength Properties of Sand-bentonite Mixtures Enhanced with Cement A. Iravanian, H. Bilsel .....	111
Improving Quality and Durability of Bitumen and Asphalt Concrete by Modification Using Recycled Polyethylene Based Polymer Composition S. Kishchynskyi, V. Nagaychuk, A. Bezuglyi .....	119
Ettringite Swelling in the Treatment of Sulfate-containing Soils Used as Subgrade for Road Constructions J. Knopp, C. Moormann .....	128
Relations between Linear ViscoElastic Behaviour of Bituminous Mixtures Containing Reclaimed Asphalt Pavement and Colloidal Structure of Corresponding Binder Blends S. Mangiafico, H. Di Benedetto, C. Sauzéat, F. Olard, S. Pouget, L. Planque .....	138
Effect of Grain Shape and Size on the Mechanical Behavior of Reinforced Sand I. Markou .....	146
Predicting the Behaviour of Fibre Reinforced Cement Treated Clay L. Nguyen, B. Fatahi, H. Khabbaz .....	153
Damage Behavior of Cement-treated Base Material K. Nusit, P. Jitsangiam .....	161
Utilization of Coal Mixed Waste Aggregates Available at Thermal Power Plants for GSB and Asphalt Mixtures Y. Pandey, Sangita, V. Tare .....	170
Long Term Cyclic Response of a Soil-cement Mixture: Experimental Study and Modelling F. Panico, A.V. da Fonseca .....	178
Silty Sand Stabilized with Different Binders S. Rios, A.V. da Fonseca, S.S. Bangaru .....	187

Recycling of CDW and Steel Slag in Drainage Layers of Transport Infrastructures A.J. Roque, P.F. da Silva, G. Rodrigues, R. Almeida	196
Assessment of Environmental Hazardous of Construction and Demolition Recycled Materials (C&DRM) from Laboratory and Field Leaching Tests Application in Road Pavement Layers A.J. Roque, I.M. Martins, A.C. Freire, J.M. Neves, M.L. Antunes	204
Damage Induced by Recycled Aggregates on the Short-term Tensile Behaviour of a High-strength Geotextile C.S. Vieira, M. de Lurdes Lopes	212
Behavior of Soil–Fly Ash–Lime Blends under Different Curing Temperatures C. Silvani, E. Braun, G.B. Masuero, N.C. Consoli	220
Numerical Analysis of Horizontal Moisture Barriers in Pavements Constructed on Expansive Soils L. Chen, R. Bulut	229
Effect of Compactness Degree on the Hydraulic Properties for Coarse Soils of High-speed Railway Embankment R. Chen, S. Qi, W. Cheng, H. Wang	237
Investigating Resilient Modulus Interdependence to Moisture for Reclaimed Asphalt Pavement Aggregates B. Cliatt, C. Plati, A. Loizos	244
Effects of Principal Stress Axis Rotation on Unsaturated Rail Track Foundation Deterioration C. Gallage, B. Dareeju, M. Dhanasekar, T. Ishikawa	252
Small Strain Behaviour of a Compacted Subgrade Soil A. Heitor, B. Indraratna, C. Rujikiatkamjorn	260
Influence of Water Content on Shear Behavior of Unsaturated Fouled Ballast T. Ishikawa, S. Fuku, T. Nakamura, Y. Momoya, T. Tokoro	268
Explanation of Dry Density Distribution Induced by Compaction through Soil/Water/Air Coupled Simulation K. Kawai, V. Phommachanh, T. Kawakatsu, A. Iizuka	276
Slope Stability Analysis Using the Unsaturated Stress Analysis. Case Study L. Batali, C. Andreea	284
Correlation between Mechanical Properties and Suction Calculated by X-ray CT of Unsaturated Sandy Soil Y. Minabe, S. Kawajiri, T. Kawaguchi, D. Nakamura, S. Yamashita	292
Characterisation of Permanent Deformation of Silty Sand Subgrades from Multistage RLT Tests F. Salour, S. Erlingsson	300
Soil Water Retention Behaviour of a Sandy Clay Fill Material D.G. Toll, J.D. Asquith, P.N. Hughes, P. Osinski	308
Numerical Simulation of Coupled Water and Salt Transfer in Soil and a Case Study of the Expansion of Subgrade Composed by Saline Soil D. Wang, J. Liu, X. Li	315
Impact of Compaction Methods on Resilient Response of Unsaturated Granular Pavement Material E. Yaghoubi, M.M. Disfani, A. Arulrajah, J. Kodikara	323
Review on Thermo-mechanical Approach in the Modelling of Geo-materials Incorporating Non-associated flow Rules Y. Aung, H. Khabbaz, B. Fatahi	331
A Retrospective View of EMM-ARM: Application to Quality Control in Soil-improvement and Complementary Developments M. Azenha, J. Silva, J. Granja, A. Gomes-Correia	339
Analysis of the Behaviour of Stone Column Stabilized Soft Ground Supporting Transport Infrastructure S. Basack, B. Indraratna, C. Rujikiatkamjorn	347
Embankment on Soft Soil Reinforced by CMC Semi-rigid Inclusions for the High-speed Railway SEA P. Burtin, J. Racinais	355
Modelling a Highway Embankment on Peat Foundations Using Transparent Soil E.M. De Guzman, M. Alfaro	363
Calibration of Resistance Factors for Load and Resistance Factor Design to Establish Value for Site Characterization D. Ding, J.E. Loehr, A. Abu El-Ela, J.J. Bowders	371
Cyclic and Post-cyclic Shear Behaviour of a Granite Residual Soil–Geogrid Interface F. Ferreira, C. Vieira, M. de Lurdes Lopes	379
Mechanical Model to Analyse Multilayer Geosynthetic Reinforced Granular Layer in Column Supported Embankments B. Ghosh, B. Fatahi, H. Khabbaz	387
Stiffness Estimation of the Soil Built-in Road Embankment on the Basis of Light Falling Weight Deflectometer Test W. Gosk	395
Soil-tunnel Interaction under Medium Internal Blast Loading Y. han, L. Zhang, X. Yang	403
Finite Difference Time Domain Simulations of Dynamic Response of Thin Multilayer Soil in Continuous Compaction Control C. Herrera, B. Caicedo	411
Investigation of the Mechanical Behaviour of the Interface between Soil and Reinforcement, via Experimental and Numerical Modelling E. Kapogianni, M. Sakellariou, J. Laue, S. Springman	419
Modelling of Plastic Culvert and Road Embankment Interaction in 3D P. Kolisoja, A. Kalliainen	427
Numerical Investigations on the Load Distribution over the Geogrid of a Basal Reinforced Piled Embankment under Cyclic Loading J. Lehn, C. Moormann, J. Aschrafi	435

In-situ Monitoring of Side Friction of Drilled Piles by Different Loading Methods L. Zhang, Y. Ma, C. Song, Y. Yang, L. Zhao	445
A New Combined Vacuum Preloading with Pneumatic Fracturing Method for Soft Ground Improvement L. Songyu, Z. Dingwen, D. Guangyin, H. Wenjun	454
Comparison of Coupled Flow-deformation and Drained Analyses for Road Embankments on CMC Improved Ground H. Mahdavi, B. Fatahi, H. Khabbaz, P. Vincent, R. Kelly	462
Driving Discomfort of MSEW and Inverted T-type Abutments M.S. Nam, J.-N. Do, J.-H. Jung, M.-C. Park	470
Bridge Pile Response to Lateral Soil Movement Induced by Installation of Controlled Modulus Columns H.H. Nguyen, H. Khabbaz, B. Fatahi, R. Kelly	475
Behavior of Soil Reinforcements in Slopes M.I. Onur, M. Tuncan, B. Evirgen, B. Ozdemir, A. Tuncan	483
Ground Improvement for a High Speed Railway Near Madrid (Spain) C.S. Oteo, J. Oteo, V. González, C. Fort	490
Improvement in Bearing Capacity of a Soft Soil by Addition of Fly Ash M.A. Ozdemir	498
Metaheuristics, Data Mining and Geographic Information Systems for Earthworks Equipment Allocation M. Parente, A.G. Correia, P. Cortez	506
Continuous Compaction Control (CCC) with Oscillating Rollers J. Pistrol, S. Villwock, W. Völkel, F. Kopf, D. Adam	514
Experimental Study on Damage Morphology and Critical State of Three-hinge Precast Arch Culvert through Shaking Table Tests Y. Sawamura, H. Ishihara, K. Kishida, M. Kimura	522
Experimental and Numerical Studies of Geotextile Encased Stone Columns in Geological Conditions of Perm Region of Russia R. Shenkman, A. Ponomaryov	530
Controlled Curved Drilling Technique in the Permeation Grouting Method for Improvement Works of an Airport in Operation S. Takano, K. Hayashi, K. Zen, R. Rasouli	539
Construction Control Chart Developed from Instrumented Trial Embankment on Soft Ground at Tokai of Kedah, Malaysia T. Yean-Chin, L. Peir-Tien, K. Kuan-Seng	548
Importance of Controlling the Degree of Saturation in Soil Compaction F. Tatsuoka, A.G. Correia	556
A Data-driven Approach for $q_u$ Prediction of Laboratory Soil-cement Mixtures J. Tinoco, A. Alberto, P. da Venda, A.G. Correia, L. Lemos	566
Two-level Structure for Tram and Road Traffic in the Centre of City-Lodz in Poland U. Tomczak, Ł. Mielczarek	574
The 2016-update of the Dutch Design Guideline for Basal Reinforced Piled Embankments S.J.M. van Eekelen	582
Piled Embankment or a Traditional Sand Construction: How to Decide? A Case Study S.J.M. van Eekelen, A.A.M. Venmans	590
Dimension Effect on $P$ - $y$ Model Used for Design of Laterally Loaded Piles M. Yang, B. Ge, W. Li, B. Zhu	598
Three-dimensional Finite Element Modelling of Soil Arching in Pile-supported Geogrid-reinforced Embankments W.-H. Zhou, J.-Y. Lao, Y. Huang, R. Chen	607
Swell-shrink Cycles of Lime Stabilized Expansive Subgrade A. Al-Taie, M.M. Disfani, R. Evans, A. Arulrajah, S. Horpibulsuk	615
2D Numerical Analysis of Shallow Foundation Rested Near Slope under Inclined Loading M. Baazouzi, D. Benmeddour, A. Mabrouki, M. Mellas	623
Constructive Constraints Regarding the Stabilization of Slopes Near Active Railway Tracks – Case Studies A. Borges, I. Pena, M. Pedrosa	635
Importance of Soil Pulverization Level in Lime Stabilized Soil Performance I. Bozbey, B. Demir, M. Komut, A. Saglik, S. Comez, A. Mert	642
Stabilizing the Landslide on Road E87 Burgas – Malko Tarnovo, Bulgaria A. Bozhinova-Haapanen	650
Behaviour of Expansive Soils Stabilized with Hydrated Lime and Bagasse Fibres L. Chi Dang, B. Fatahi, H. Khabbaz	658
Multiojective Optimization of Maintenance Scheduling: Application to Slopes and Retaining Walls R. Denysiuk, J.C. Matos, J. Tinoco, T. Miranda, A.G. Correia	666
Application of the Upper and Lower-bound Theorems to Three-dimensional Stability of Slopes N. Deusdado, A.N. Antão, M.V. da Silva, N. Guerra	674
The Impact of Freezing-thawing Process on Slope Stability of Earth Structure in Cold Climate A.A. Korshunov, S.P. Doroshenko, A.L. Nevzorov	682
Landslide Hazard Assessment for National Rail Network K.A. Freeborough, D. Diaz Doce, R. Lethbridge, G. Jessamy, C. Dashwood, C. Pennington, H.J. Reeves	689

The Implications of Using Estimated Solar Radiation on the Derivation of Potential Evapotranspiration and Soil Moisture Deficit within an Embankment	
P. Helm, R. Stirling, S. Glendinning	697
Using Remote Sensing Techniques to Identify the Landslide Hazard Prone Sections along the South Link Railway in Taiwan	
C.-H. Hsu, T.-C. Tsao, C.-M. Huang, C.-F. Lee, Y.-T. Lee	708
Slope Stability Assessment and Evaluation of Remedial Measures Using Limit Equilibrium and Finite Element Approaches	
M. Neves, V. Cavaleiro, A. Pinto	717
Development of an Evidence-based Geotechnical Asset Management Policy for Network Rail, Great Britain	
C. Power, J. Mian, T. Spink, S. Abbott, M. Edwards	726
The Implementation of Geotechnical Data Into the BIM Process	
L.R. Tawelian, S.B. Mickovski	734
Lomé Container Terminal	
R. Tomásio, A. Pinto, C. Cota, P. Rosa, M. Figueres	742
Stability of Slopes and Embankments of Coarse Man-made Soils	
V. Vyrozhemsky, I. Voloshyna	750
A Strategic Approach to Debris flow Risk Reduction on the Road Network	
M.G. Winter	759
Preliminary Testing on High-speed Railway Substructure Due to Water Level Changes	
X. Bian, H. Jiang, Y. Chen	769
On the Use of Geophones in the Low-frequency Regime to Study Rail Vibrations	
I. Crespo-Chacón, J.L. García-de-la-Oliva, E. Santiago-Recuerda	782
A Double-layered Model for Highway Subgrade and its Dynamic Response due to Traffic Loads	
L. Fu, J. Zhou, W. Wang, J. Wang	795
Compaction Control of Clayey Soils Using Electrical Resistivity Charts	
V. Gingine, A.S. Dias, R. Cardoso	803
Effect of the Principal Stress Direction on Cyclic Cumulative Deformation and Pore Pressure of Soft Clay	
M. Huang, Z. Yao	811
3D Finite Element Model as a Tool for Analyzing the Structural Behavior of a Railway Track	
A. Kalliainen, P. Kolisoja, A. Nurmikolu	820
Effects of Freeze-thaw History on Bearing Capacity of Granular Base Course Materials	
S. Kawabata, T. Ishikawa, S. Kameyama	828
Laboratory Examination of Frost-heaving Properties of Road Unbound Mixtures Based on Fines Content and Plasticity Index	
C. Kraszewski, L. Rafalski	836
Design of Thin Surfaced Asphalt Pavements	
S. Leischner, F. Wellner, G.C. Falla, M. Oeser, D. Wang	844
Study of Permanent Deformation and Granulometric Distribution of Graded Crushed Stone Pavement Material	
C. Lima, L. Motta	854
Correlating Nonlinear Parameters of Resilient Modulus Models for Unbound Geomaterials	
M. Mazari, I. Abdallah, J. Garibay, S. Nazarian	862
Instrumentation Techniques for Studying the Horizontal behavior of High-speed Railways	
J. Moreno-Robles, I. Crespo-Chacón, J.L. García-de-la-Oliva	870
Impact of Dual Gauge Railway Tracks on Traffic Load Induced Permanent Deformation of Low Embankments	
A.D. Mwanza, P. Hao, M. Muya, Z. Haiwei	880
A Numerical Study on the Implications of Subgrade Reinforcement with Geosynthetics in Pavement Design	
J. Neves, H. Lima, M. Gonçalves	888
Mechanical Stabilization of Unbound Layers to Increase Pavement Performance and Incorporation of Benefits into M-E Analysis	
T. Oliver, M. Wayne, J. Kwon	896
A Framework to Utilize Shear Strength Properties for Evaluating Rutting Potentials of Unbound Aggregate Materials	
I. Qamhia, E. Tutumluer, L.C. Chow, D. Mishra	911
Modelling the Moisture Dependent Permanent Deformation Behavior of Unbound Granular Materials	
M.S. Rahman, S. Erlingsson	921
Influence of Post Compaction on the Moisture Sensitive Resilient Modulus of Unbound Granular Materials	
M.S. Rahman, S. Erlingsson	929
Deformation Modelling of Instrumented Flexible Pavement Structure	
T. Saevarsdottir, S. Erlingsson	937
Nondestructive Deflection Testing Based Mechanistic-empirical Overlay Thickness Design Approach for Low Volume Roads: Case Studies	
P. Sarker, E. Tutumluer, S. Lackey	945
An Elasto-plastic Method for Analysing the Deformation of the Railway Ballast	
Q. Sun, B. Indraratna, S. Nimbalkar	954
Feasibility of Using 4 <sup>th</sup> Power Law in Design of Plastic Deformation Resistant Low Volume Roads	
V. Emre UZ, M. Saltan, İ. Gökalp	961
A Comparison between a Shakedown Design Approach and the Analytical Design Approach in the UK for Flexible Road Pavements	
J. Wang, S. Liu, H.-S. Yu	971

Performance Checks for Unbound Aggregate Base Permanent Deformation Prediction Models under Dynamic Stress States Induced by Moving Wheel Loading	
Y. Xiao, E. Tutumluer	979
Microstructure Study on Intact Clay Behavior Subjected to Cyclic Principal Stress Rotation	
L. Qinghui, Y. Jiajia, Z. Jian, C. Zhigang	991
A Review and Evaluation of Ballast Settlement Models Using Results from the Southampton Railway Testing Facility (SRTF)	
T. Abadi, L. Le Pen, A. Zervos, W. Powrie	999
Assessment of Interface Shear Behaviour of Sub-ballast with Geosynthetics by Large-scale Direct Shear Test	
M.M. Biabani, B. Indraratna, S. Nimbalkar	1007
Quantifying Degradation of Railway Ballast Using Numerical Simulations of Micro-deval Test and In-situ Conditions	
I. Deiros, C. Voivret, G. Combe, F. Emeriault	1016
Dynamic Characterization of the Supporting Layers in Railway Tracks Using the Dynamic Penetrometer Panda 3®	
E. Escobar, M.B. Navarrete, R. Gourvès, Y. Haddani, P. Breul, B. Chevalier	1024
Critical Velocity of High-speed Train Running on Soft Soil and Induced Dynamic Soil Response	
J. Hu, X. Bian, J. Jiang	1034
Remediation of Mud Pumping on a Ballasted Railway Track	
A. Hudson, G. Watson, L. Le Pen, W. Powrie	1043
Problems with Railway Track Drainage in Finland	
J. Latvala, A. Nurmikolu, H. Luomala	1051
Dynamic Performance of Pile-supported Bridge-embankment Transition Zones Under High-speed Train Moving Loads	
W. Li, X. Bian	1059
Discrete Element Analysis of Railway Ballast under Cycling Loading	
E. Mahmoud, A.T. Papagiannakis, D. Renteria	1068
Proving MEMS Technologies for Smarter Railway Infrastructure	
D. Milne, L. Le Pen, G. Watson, D. Thompson, W. Powrie, M. Hayward, S. Morley	1077
Deformation Characteristics of Track Structures for Level Crossings Subjected to Heavy Forklift Load	
Y. Momoya, K. Ito	1085
Numerical Investigations on Track-substructure System Considering the Effect of Different Train Speeds	
C. Moormann, J. Lehn, J. Aschrafi, D. Sarkar	1093
Shaking Table Test Using Full-scale Model for Lateral Resistance Force of Ballasted Tracks During Earthquake	
T. Nakamura, Y. Momoya, K. Nomura, Y. Yoshihiko	1100
Application of Shock Mats in Rail Track Foundation Subjected to Dynamic Loads	
S.K. Navaratnarajah, B. Indraratna, S. Nimbalkar	1108
Railway Ballast: Grain Shape Characterization to Study its Influence on the Mechanical Behaviour	
N. Ouhbi, C. Voivret, G. Perrin, J.-N. Roux	1120
Non-linear Behaviour of Geomaterials in Railway Tracks under Different Loading Conditions	
A. Paixão, J.N. Varandas, E. Fortunato, R. Calçada	1128
The Vibration Impact of Heavy Freight Train on the Roadbed	
A. Petriaev	1136
Construction of the New High-speed Railway Line Ulm–Wendlingen in Karstified Rock	
M. Raithel, J. Baumbusch, S. Kielbassa	1144
Investigation into Impact of Train Speed for Behavior of Ballasted Railway Track Foundations	
M. Abu Sayeed, M.A. Shahin	1152
Some Predictions of Deformations from Tram Track Construction in a Structure-Embankment Transition Zone	
Y. Shan, S. Zhou, Q. Gong, J. Xiao, C. Wang, X. Zhang, S. Xu, Z. Yu	1160
A Numerical Study on the Stress Changes in the Ballast Due to Train Passages	
J.N. Varandas, A. Paixão, E. Fortunato, P. Hölscher	1169
Modeling Behaviour of Railway Ballast in Prismoidal Apparatus Using Discrete Element Method	
G.C. Vizcarra, S. Nimbalkar, M. Casagrande	1177
Influences of Subgrade Form and Ground Stiffness on Dynamic Responses of Railway Subgrade under Train Loading: Field Testing Case Study	
J. Xiao, B. Wang, C. Liu, Z. Yu	1185
Railways Track Characterization Using Ground Penetrating Radar	
S. Fontul, E. Fortunato, F. De Chiara, R. Burrinha, M. Baldeiras	1193
Trackbed Mechanical and Physical Characterization Using PANDA®/Geoendoscopy Coupling	
Y. Haddani, P. Breul, G. Saussine, M.A.B. Navarrete, F. Ranvier, R. Gourvès	1201
The Impact of Unfrozen Water Content on Ultrasonic Wave Velocity in Frozen Soils	
L. Dongqing, H. Xing, M. Feng, Z. Yu	1210
Development of Smart Braided Structures for Sensing of Geotechnical Structures	
S. Rana, R. Fangueiro, A.G. Correia	1218
A Condition Assessment Approach for Highway Filter Drains Using Ground Penetrating Radar	
T. Stylianides, M.W. Frost, P.R. Fleming, M. Mageean, A. Huetson	1226

Soil Formation Lithological Profiling Using Ground Penetrating Radar Y.A. Sukhobok, V.V. Pupatenko, G.M. Stoyanovich, Y.V. Ponomarchuk	1236
Rapid and Non-intrusive Measurements of Moisture in Road Constructions Using Passive Microwave Radiometry and GPR – Full Scale Test A.A.M. Venmans, R. van de Ven, J. Kollen	1244
Nanotechnology Applied to Chemical Soil Stabilization A.A.S. Correia, M.G. Rasteiro	1252
Evaluation of Asphalt Binders Modified with Nanoclay and Nanosilica H. Ezzat, S. El-Badawy, A. Gabr, E.-S. Ibrahim Zaki, T. Breakah	1260
The Soil and Groundwater Remediation with Zero Valent Iron Nanoparticles J.R. Gonçalves	1268
Rheological Evaluation of Asphalt Cements Modified with ASA Polymer and $Al_2O_3$ Nanoparticles M. Mubarak, S.I. Albrka Ali, A. Ismail, N.I. Md. Yusoff	1276
DEM Analysis of Railtrack Ballast Degradation under Monotonic and Cyclic Loading J. Qian, J. Gu, X. Gu, M. Huang, L. Mu	1285
Dynamic Shakedown Analysis of Flexible Pavement under Traffic Moving Loading J. Qian, Y. Wang, Z. Lin, Y. Liu, T. Su	1293
Biostabilization of a Sandy Soil Using Enzymatic Calcium Carbonate Precipitation J.P.S.F. Carmona, P.J.V. Oliveira, L.J.L. Lemos	1301
Developing a Performance Criteria for Stone Columns to Improve Surface Pavement for Weak Subgrade Conditions S.F. Ibrahim, N.G. Ahmed, D.E. Mohammed	1309
Using Blends of Construction & Demolition Waste Materials and Recycled Clay Masonry Brick in Pavement A. Arisha, A. Gabr, S. El-Badawy, S. Shwally	1317
Parametric Study of Applied Stresses on Infiltration Modular Cells Installed under Roads T.H. Aung, H. Khabbaz, B. Fatahi	1325
On the Exploitation of Ground Heat Using Transportation Infrastructure P. Bourne-Webb, R. da Costa Gonçalves	1333
A Numerical Study on the Critical Height of Embankments Supported by Geotextile Encased Granular Columns M. Carreira, M. Almeida, A. Pinto	1341
Numerical Study of High Speed Railway Subgrade Settlement Induced by Underwater Lowering R. Chen, W. Cheng, R. Jia, S. Qi, H. Wang	1350
The Impact of the Type and Technical Condition of Road Surface on the Level of Traffic-generated Vibrations Propagated to the Environment K.R. Czech	1358
Remediation of Expansive Soils Using Agricultural Waste Bagasse Ash H. Hasan, L. Dang, H. Khabbaz, B. Fatahi, S. Terzaghi	1368
An Analytical Model of PVD-assisted Soft Ground Consolidation B. Indraratna, R. Zhong, C. Rujikiatkamjorn	1376
Geotechnical Design and Construction of Improvements to Existing Railway Lines M. Neves, C. Holt, R. McConnell, G. Marjane	1384
Colombian Soil Stabilized with Geopolymers for Low Cost Roads S. Rios, C. Ramos, A.V. da Fonseca, N. Cruz, C. Rodrigues	1392
Sustainable Development in Transport Construction through the Use of the Geocoprotective Technologies A. Sakharova, L. Svatovskaya, M. Baidarashvili, A. Petriaev	1401
Rutting Behavior of Geocell Reinforced Base Layer Overlying Weak Sand Subgrades V.V. Kumar, S. Saride	1409
Added Value of Transportation Geotechnics to the Sustainability (Design Approach) I. Vaníček, D. Jirásko, M. Vaníček	1417
The Economic Impact of Landslides and Floods on the Road Network M.G. Winter, B. Shearer, D. Palmer, D. Peeling, C. Harmer, J. Sharpe	1425
Problems with Landslide Stabilization of Dukat in the Road Vlora – Saranda L. Bozo, K. Cela	1435
The Performance of Road Embankments on Glacial Deposits in Ireland F. Buggy, P. Kissane	1443
Case Study: Preliminary Field Testing as a Basis of Design for Ground Improvement Using Vibrocompaction at Lomé Container Terminal-Togo A. Cristovao, M. Figueres, A. Pinto, P. Rosa	1451
Analysis of the Vibration Propagation Induced by Pulling out of Sheet Pile Wall in a Close Neighbourhood of Existing Buildings K. Czech, W. Gosk	1460
CDC Compaction at Berth 9 Quay Extension Felixstowe, UK J.W. Vink, J.W. Dijkstra	1468
Study on Sliding Characteristics and Controlling Measures of Colluvial Landslides in Qinghai-Tibet Plateau H. Tian-fei, L. Jian-kun, Z. Ben-zhen, Z. Jing	1477
Field Assessment of Ballasted Railroads Using Geosynthetics and Shock Mats S. Nimbalkar, B. Indraratna	1485

Ground Improvement with Jet Grouting Solutions at the New Cruise Terminal in Lisbon, Portugal A. Pinto, R. Tomásio, G. Marques . . . . .	1495
San Pasquale Station of Line 6 in Naples: Measurements and Numerical Analyses G. Russo, M.V. Nicotera, S. Autuori . . . . .	1503
Rehabilitation and Reinforcement of the Marina Expo Breakwaters, Lisbon, Portugal R. Tomásio, A. Pinto, J. Pernão . . . . .	1511
Engineering Test Research of XPS Insulation Structure Applied in High Speed Railway of Seasonal Frozen Soil Roadbed D. Cai, H. Yan, J. Yao, Y. Cui, F. Chen. . . . .	1519





# Soil Formation Lithological Profiling Using Ground Penetrating Radar

Yuri A. Sukhobok, Viktor V. Pupatenko, Gennady M. Stoyanovich and  
Yulia V. Ponomarchuk

*Far Eastern State Transport University, Khabarovsk, Russia  
yuri.sukhobok@gmail.com*

## Abstract

The paper presents a modified technique for generation of the high-contrast sub-horizontally layered earth depth sections which is based on the common offset and common midpoint GPR methods. The iterative algorithm for fitting and correction of the reflection and refraction time-distance curves, as well as identification of the basic layer parameters, is suggested. Some results of the technique's implementation on railroads and highways in the Russian Far East are summarized.

**Keywords:** Ground penetrating radar, common-offset reflection survey, wide angle reflection and refraction method, geotechnical investigations, data processing

## 1 Introduction

One of the most widely recommended method of geophysical survey is a ground-penetrating radar (GPR). It is based on radio frequency broadband signal emission into medium by a transmitter and response signal registration by a receiver. The response signal is a superposition of amplitudes of forward, reflected, and refracted waves, which reach a receiving antenna.

One of the important GPR applications in surveys of transportation facilities subsurface or subgrade is construction of a depth section of the surveyed medium. Generally the medium is non-uniform, however, it can be considered to be constructed of uniform subhorizontal layers of finite quantity with precision, which is sufficient for practical use. According to this model the electrophysical properties of ground layers change step-wise. For instance, filled and foundation soils in different conditions (watered, thawed out or frozen), engineering structures, reinforced, insulating, and separating layers and constructions can be found in subgrade surveys of railroads and highways, runways and other structures.

In order to construct a depth section of an extensive site usually GPR survey is conducted. A linear profile is marked on the surveyed area and a GPR unit, which has a constant distance between its transmitting and receiving antennae, is moved from one point to another within a given step along it. At each point a signal (trace) is registered. Signals, received from all the points, form a radargram.

The main problems of a camera treatment are as follows: detection of interface boundaries on a radargram and detection of the depths, where these boundaries are located. The first problem, which was thoroughly studied in [1, 2], is out of the scope of this paper. It is further assumed that the interface boundaries are detected previously. The goal of this research is to advance the detection technique of depths, where the interface boundaries are located, that is transformation technique of the source reflection-time section to the depth section.

## 2 Related Work on Transformation Techniques of the Source Reflection-Time Section to the Depth Section

In order to transform the source reflection-time section to the depth section, first of all, it is necessary to calculate the velocity of electromagnetic wave propagation in each layer (strata velocity). Since the reflected signal propagates through the whole ground layers, in order to evaluate the strata velocity in a given stratum the notion of a root-mean-square (RMS) velocity is introduced. It represents the mean velocity of electromagnetic signal propagation at a given point on the ground surface (emission source) to a given point of ground depth. The strata and RMS velocities are related to each other.

Nowadays a few techniques have been developed in order to estimate RMS velocities and, therefore, strata velocities. The simplest method relies on velocity calculation according to the diffraction curves [2]. Its idea is based on the fact that if there are local diffractors in the section area (big rocks, pipes, cables), the curve of arrival time versus distance has a hyperbolic form on the GPR radargram.

The disadvantage of this technique is that in order to have a success in its implementation a sufficient number of local diffractors are needed to be situated in different depths. Frequently these objects are located only in the upper layer of the section and non-uniformly along the profile length. The forms of hyperbolic time-distance curves are not reliably detected when there is a large interference that leads to errors in velocity estimation.

Another technique for estimation of the signal propagation velocities in different strata is based on amplitude fluctuations on strata boundaries [4]. The main drawback of the method is the measurement complexity of the decaying signal amplitude, which leads to significant errors with the increase of the reflecting boundary depth. Moreover, there may be no significant change in amplitude values on the boundaries of layers when the dielectric constants of ground layers change insignificantly. In the meantime due to interference and re-reflections “false” jumps may occur, which do not depend on the ground layers boundary surfaces.

The next method is based on direct velocity measurement with the help of the common-midpoint (CMP) or the wide angle refraction and reflection mode (WARR) techniques. According to these techniques, the distance between the antennae increases from 0 to a maximum value, usually up to 10 meters. It should be noted that the CMP technique operates with the both antennas which are moved equidistantly from the midpoint. However according to the WARR technique the position of the one antenna is fixed while the other one is moved step-by-step away from the fixed one. According to both methods an electromagnetic impulse is generated and then a signal is registered at the receiving antenna at each point of measurement. The types of waves representing the received signal can be classified as direct, refracted and reflected ones. These waves could be represented in the form of the time-distance curves. These curves are detected from the radargram (Fig. 1).

Generally the CMP technique is more accurate than WARR for obtaining velocity. The cause of this difference is that moving both antennas equidistantly from the midpoint ensures that the average velocity is being measured using the same reflection interface, at the same location. Since the reflection surfaces of subgrade are assumed horizontal, the WARR technique could be used for a subgrade survey. In addition, the recording surface is horizontal in the longitudinal direction, for subgrade surface and

berms, which allow to conduct WARR tests. This technique, in addition, is two times faster than CMP for the considered types of GPR units.

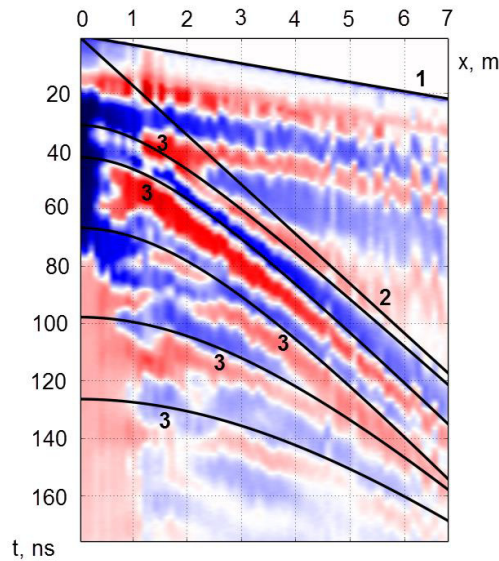


Fig.1. An example of radargram, which was obtained after the WARR measurement. Rectilinear time-distance curves of direct air wave (1), direct ground wave (2) and hyperbolic time-distance curves of reflected waves (3) are detected;  $x$  – the axis of distance between the antennae, m.

The time-distance curves of reflected waves are approximated by hyperbolic functions, and for each of them a corresponding equation can be found. If it is assumed that the trajectories of beams are rectilinear (i.e., do not change while propagating from one medium to another), then the time-distance curve equation is expressed in engineering seismicity as [6]:

$$t_{\text{refl}-n}(x) = \frac{1}{V_{\text{stack}}} \sqrt{4H_n^2 + x^2}, \quad (1)$$

where  $t_{\text{refl}-n}$  – is a 2-way time of reflected wave propagation, ns;  $x$  – distance between antennae, m;  $H_n$  – depth of  $n$ th layer's top, m;  $V_{\text{stack}}$  – stacking velocity of electromagnetic waves propagation in the medium; in this case it is equal to the RMS velocity of electromagnetic waves propagation in the medium from the surface to the top of the  $n$ th layer  $V_{\text{RMS}}$ , m/ns.

The estimation of the RMS velocities of electromagnetic waves propagation and boundary depths leads to the problem of the coefficients fitting in equation (1). These values can be adjusted by time-distance curves approximation of the direct and refracted waves. Then, the each layer thickness is evaluated according to the estimated strata velocities.

One significant drawback of this method is based on assumption that the beam trajectories are rectilinear. However, when propagating from one layer to another the beams are refracted and, therefore, deviate from the initial direction.

Therefore the technique can be used only for media, in which the velocities of electromagnetic waves propagation do not differ more than by 10-15% from each other. If a surveyed ground area significantly differs in velocities, the deviation of the beam trajectory from a straight line can not be neglected.

The technique, which is based on WARR results processing, is versatile. In the simplest implementation this method does not allow to estimate the ground model with significant velocity

variation between different layers. Therefore the goal of this research was to modify the transformation of the source reflection-time section into depth section according to the results of the WARR technique without the mentioned constraint.

### 3 Modification of the Transformation Technique of the Source Reflection-Time Section into Depth Section according to the WARR technique

Let us consider the model of reflected wave propagation in a multilayered medium, which consists of separate homogeneous layers with horizontal boundaries (Fig. 2).

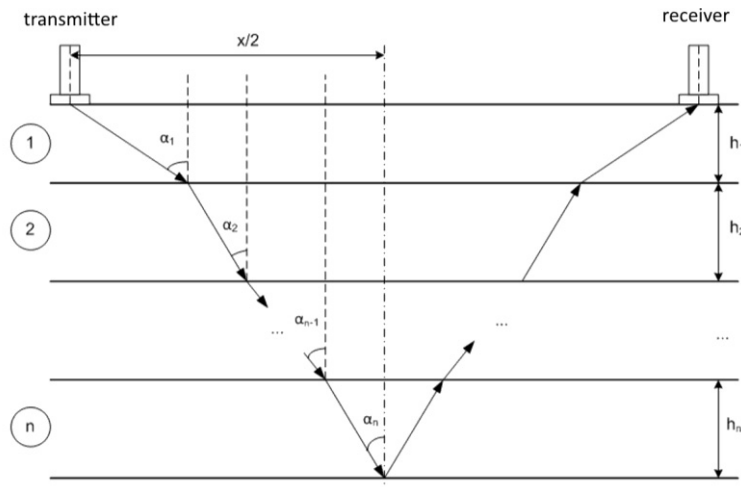


Fig. 2. The scheme of reflected wave propagation in a multilayered medium with horizontal boundaries:  $x$  – the distance between the antennae, m;  $h_i$  – the thickness of the  $i$ th layer, m.

In [5] it was shown that the time-distance curves cease to have hyperbolic form according to this model (Fig. 5, a). Their equation can be defined in parametric form:

$$\begin{cases} t_n(p) = 2 \sum_{i=1}^n \frac{h_i}{V_i \cdot \sqrt{1 - p^2 V_i^2}} \\ x_n(p) = 2 \sum_{i=1}^n \frac{p \cdot h_i \cdot V_i}{\sqrt{1 - p^2 V_i^2}} \end{cases}, \quad (2)$$

where  $n$  is the number of layers;  $V_i$  – the velocity of electromagnetic wave propagation in the  $i$ th layer (stratum velocity), m/ns;  $h_i$  – the  $i$ th layer thickness, m;  $p$  – ray parameter, which is defined according to the following expression:

$$p = \frac{\sin \alpha_1}{V_1} = \frac{\sin \alpha_2}{V_2} = \dots = \frac{\sin \alpha_n}{V_n}, \quad (3)$$

where  $\alpha_1, \alpha_2, \dots, \alpha_n$  – the angles of incidence in the first, second, ..., and  $n$ th layers respectively.

It was shown in [6] that it is impossible to obtain the expressions to calculate the strata velocity from (2). Moreover, equation (2) can not be represented in non-parametric form, as an expression  $t = f(x)$ .

This makes sure that it is impossible to evaluate adequate values of parameters for equation (2) on the basis of a selected time-distance curve and, therefore, precise computing of velocity values.

The technique, which uses the limiting efficient velocity, is used in engineering seismicity in order to estimate the strata velocities approximately [5]. This method is based on hyperbolic approximation of curve (2). According to expression (2) an effective velocity  $V_{stack}$  is obtained, which is not equal to the RMS velocity and which can not be transformed into the strata velocities.

However the author of [5] showed that with the approach to the time-distance curve axis, in the section of which the space between the antennae is equal to 0, the effective velocity is called the limiting effective velocity:  $V_e = \lim_{x \rightarrow 0} V_{\alpha\phi}(x)$  and it can be used to estimate the strata velocities using Dix formula [5]:

$$V_i = \sqrt{\frac{V_{e(i)}^2 \cdot t_{0(i)} - V_{e(i-1)}^2 \cdot t_{0(i-1)}}{t_{0(i)} - t_{0(i-1)}}}, \quad (4)$$

where  $V_{e(i)}$  is the limiting efficient velocity according to hyperbolic form of the approximation of the time-distance curve of the wave, which is reflected from  $i$ th layer, m/ns;  $t_{0(i)}$  – double signal propagation time of the wave, which was reflected from the boundary between  $i$ th and  $(i+1)$ th layers (which corresponds to the vertex of the hyperbola of the reflected wave), ns;  $V_{e(i-1)}$  and  $t_{0(i-1)}$  – the same values at  $(i-1)$ th layer.

Therefore, the limiting effective velocity  $V_e$  can be estimated, if the hyperbolic approximation is applied not to the whole time-distance curve of reflected waves, but to its part, which is the closest to its axis. Let us denote this approximating hyperbola as a *conditional time-distance curve* (Fig. 3, b). The ground model is developed according the conditional time-distance curves: the velocities of signal propagation in the layers, as well as the layer thicknesses, are computed.

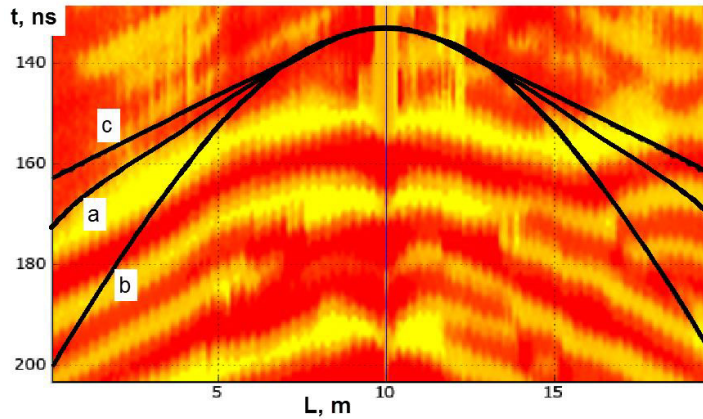


Fig. 3. A fragment of a radargram, which was obtained after the WARR measurement: a – the form of the original non-hyperbolic time-distance curve of the reflected wave; b – the conditional hyperbolic time-distance curve; c – the estimated time-distance curve.

On the basis of the technique, described above, an iterative algorithm was developed, which is based on step-by-step approximation of the ground model parameters  $\{h_i, V_i\}$ . According to the current values of the model parameters equation (4) is resolved numerically with respect to  $x$  and  $t$  (a direct geophysical problem is solved – an approximation of a *calculated time-distance curve* according to the ground model data). The solution of this equation consists of finding such values of angle  $\alpha_1$  and, consequently,

parameter  $p$ , so that the value of  $x$  is to be equal to the corresponding distance between the antennae. By considering all the distance values between the antennae from 0 to the maximum value and solving numerically equation (4), a set of points  $(x_j, t_j)$  can be obtained for  $0 \leq x_j \leq x_{max}$ . These points form the calculated time-distance curve (Fig. 3, c), which is to be compared to the actual time-distance curve. If the calculated and the actual time-distance curves do not coincide, it is necessary to correct the conditional time-distance curve and solve again the inverse and direct geophysical problems.

If some a priori data on any layer thickness and velocity of electromagnetic wave propagation in any medium is available, it is necessary to introduce corrections into the ground model before solving the direct problem.

The iterative process is repeated till the actual and calculated time-distance curves coincide with sufficient accuracy. Methods of mathematical statistics, for example, the least square method are applied in order to minimize the residual.

The last stage is to transform the time section into the depth section according to the ground model. It is necessary to mark layer boundaries according to the estimated velocities of electromagnetic waves propagation in ground layers. This step is also implemented using the numerical solution of equation (2) separately for each GPR position and each boundary.

## 4 The Results of the Technique Implementation for the Transport Infrastructure Facilities

The proposed technique was implemented to survey various earth structures of the Russian Far East transportation facilities.

For example, the geophysical monitoring of the railway subgrade formation settlements was carried out at Kuznetsovo, Nakhodka – Khmilovsky section of the Far Eastern Railway in 2009 – 2011. The GPR units LOZA-N and LOZA-V were used provided with antennae, which have band center frequency from 25 to 100 MHz.

The WARR tests were carried out on the subgrade surface and the subgrade berms in the longitudinal direction. The test results were processed according to the proposed method (Fig. 4). As a result the ground model was developed and the ground profile of the subgrade formation settlements was obtained as longitudinal and cross-sectional profiles (Fig. 4). These results allowed detecting the locations of the maximum subsidence and monitoring the dynamics of soil settlements changes within the observation period. Moreover, the design decision – the placing of geotextile layers, was detected.

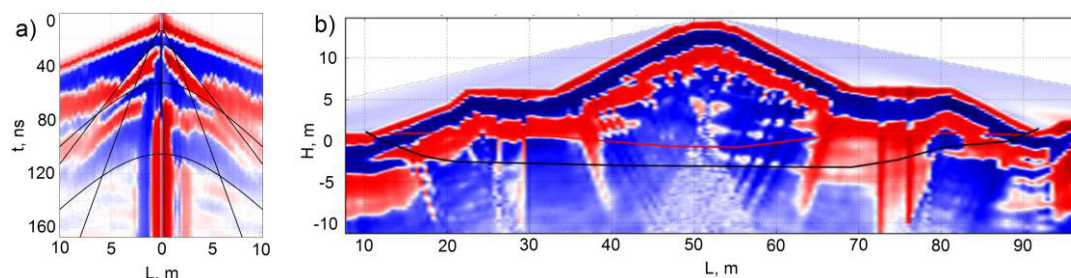


Fig. 4. The results of the geophysical survey of the railway subgrade formation settlements which was carried out at Kuznetsovo, Nakhodka – Khmilovsky section of the Far Eastern Railway: a – the radargram, obtained by the WARR measurement; b – GPR profile along the cross-section of the subgrade formation.



The highway monitoring in the Khabarovsk Territory of Russia was carried out in 2013. In order to conduct the survey the following GPR units were used: LOZA, OKO-2, and MALA GeoScience CX-11, provided with antennae of various frequencies (15-1700 MHz). The common-offset survey was carried out along the cross-sectional and longitudinal profiles. The distance between antennae was set to one meter. The multi-offset acquisition was also conducted at the specific points on the road surface.

The application of the proposed technique allowed obtaining a lithological section of the surveyed media. The results of comparison of borehole data with GPR data (Fig. 5) are satisfying generally. The occurrence of the second and the third reflection surface could be explained as at the discrepancy of the mineral composition of soils.

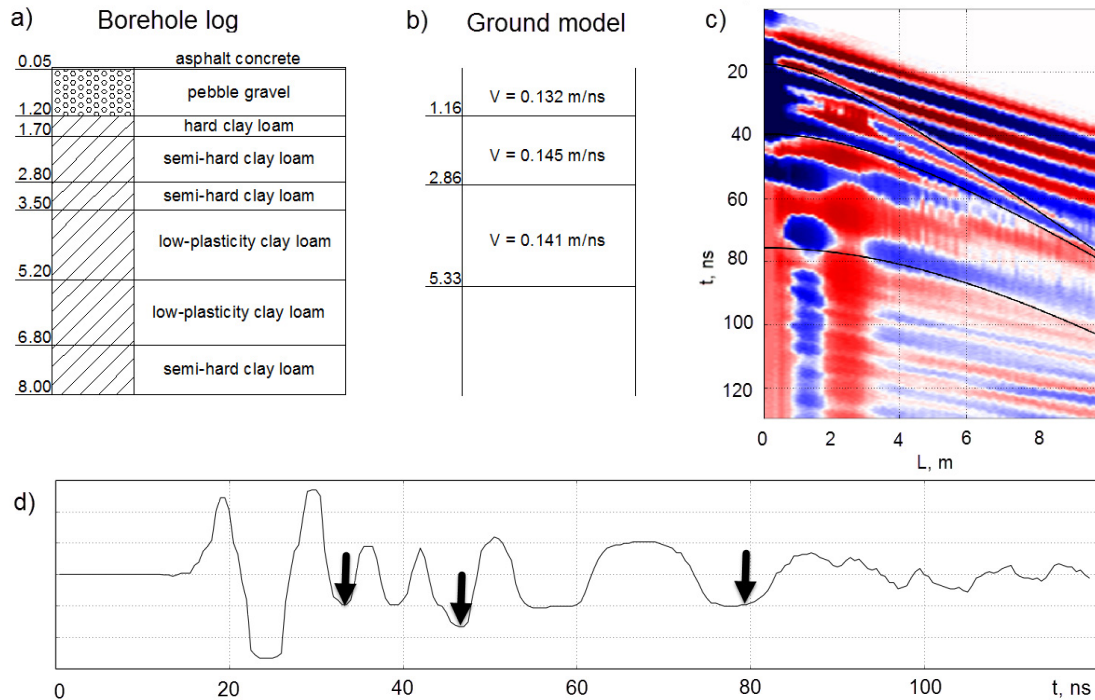


Fig. 5. The borehole data compared to the GPR data (highway section near Mukhen settlement): a – borehole log; b – ground model; c – radargram with marked time-distance curves of the reflected waves; d – the example of the GPR trace with 3.8 m offset: arrival time of the wavefronts is indicated by the arrows.

## 5 Conclusion

The research results allowed developing a technique for the heterogeneous media boundaries detection in order to do the lithological profiling of geological section. Besides the experiments on transport facilities presented in the previous section, the proposed technique was also tested in order to detect boundaries of filled-up ground while laying foundation, foundation pit contouring, displacement surface of downslopes, etc. The experience of implementation has shown that the integral use of traditional geotechnical methods (boring, test pit sampling) and geophysical methods (ground penetrating radar, seismic, etc.) allows providing the reliability of results and reducing labor costs and labor hours of geotechnical survey during construction of new facilities or reconstruction of objects, which are maintained for a long time.

## References

- [1] Daniels DJ, editor. *Ground Penetrating Radar*. London: the Institution of Electrical Engineers; 2009.
- [2] Grinev AI. The Ground Penetrating Radar Problems, 2005 [Voprosi podpoverkhnostnoy radiolokatsii], Radiotekhnika, Moscow, 2005, 416 p.
- [3] Huisman JA, Hubbard SS, Redman JD, Annan AP. Measuring Soil Water Content with Ground Penetrating Radar: A Review. *Vadose Zone Journal* 2003; issue 2; p. 476-491.
- [4] Huang C., Su Y. A new GPR calibration method for high accuracy thickness and permittivity measurement of multi-layered pavement. *Tenth International Conference of Ground Penetrating Radar* 21-24 June, 2004; p. 627-630.
- [5] Gurvich II, Nomokonov VP. *The exploration seismology. Geophysics handbook* [Seysmorazvedka. Spravochnik geofizika]. Moscow: Nedra; 2001, p. 105-106.
- [6] Yilmaz O. *Seismic data analysis*. 2nd edition. Volume 1. Tulsa: Society of Exploration Geophysicists; 2001.